

# Comparison of Noncontrast MRI Magnetization Transfer and $T_2$ -Weighted Signal Intensity Ratios for Detection of Bowel Wall Fibrosis in a Crohn's Disease Animal Model

Jonathan R. Dillman, MD,<sup>1\*</sup> Scott D. Swanson, PhD,<sup>2</sup> Laura A. Johnson, BS,<sup>3</sup>  
David S. Moons, MD, PhD,<sup>4</sup> Jeremy Adler, MD, MS,<sup>5</sup> Ryan W. Stidham, MD,<sup>3</sup>  
and Peter D.R. Higgins, MD, PhD<sup>3</sup>

**Purpose:** To compare the abilities of magnetization transfer magnetic resonance imaging (MT-MRI) and  $T_2$ -weighted signal intensity ( $T_2$ WSI) ratios to detect intestinal fibrosis in a Crohn's disease animal model.

**Materials and Methods:** Ten rats ("Group 1") received one trinitrobenzenesulfonic acid enema to induce acute colonic inflammation, while 10 additional animals ("Group 2") received multiple enemas to induce colonic inflammation and fibrosis. Gradient recalled-echo MT-MRI (5 and 10 kHz off-resonance) and  $T_2$ -weighted spin-echo imaging were performed 2 days after the last enema. MT ratios (MTR) and  $T_2$ WSI ratios were calculated in the area of greatest colonic thickening. Bowel wall MTR, bowel wall MTR normalized to paraspinous muscle MTR ("normalized MTR"), and  $T_2$ WSI ratios were compared between animal groups using Student's *t*-test.

**Results:** At 10 kHz off-resonance, mean bowel wall MTR for Group 1 was  $24.8 \pm 3.1\%$  vs.  $30.3 \pm 3.2\%$  for Group 2 ( $P = 0.001$ ). Mean normalized MTR was  $0.45 \pm 0.05$  for Group 1 and  $0.58 \pm 0.08$  for Group 2 ( $P = 0.0003$ ). At 5 kHz off-resonance, mean bowel wall MTR for Group 1 was  $34.7 \pm 5.2\%$  vs.  $40.3 \pm 3.6\%$  for Group 2 ( $P = 0.015$ ). Mean normalized MTR was  $0.53 \pm 0.08$  for Group 1 and  $0.64 \pm 0.07$  for Group 2 ( $P = 0.003$ ). Mean  $T_2$ WSI ratio was  $5.32 \pm 0.98$  for Group 1 and  $3.01 \pm 0.66$  for group 2 ( $P < 0.0001$ ). Mean  $T_2$ WSI ratio/MTR (10 kHz off-resonance) was  $12.06 \pm 2.70$  for Group 1 and  $5.22 \pm 1.29$  for Group 2 ( $P < 0.0001$ ), with an ROC c-statistic of 0.98.

**Conclusion:** MTR and  $T_2$ WSI ratios detect bowel wall fibrosis in a Crohn's disease animal model.

J. MAGN. RESON. IMAGING 2015;42:801–810.

Crohn's disease (CD) is a segmental granulomatous inflammatory bowel disease that affects about 600,000 children and adults in the United States, is associated with substantial morbidity and healthcare costs, and is commonly characterized by recurring periods of exacerbation and remission.<sup>1–3</sup> Over time, repeated bowel wall injury due to acute and chronic inflammation and related attempts at healing can unpredictably result in the deposition of fibrous tissue

(scar).<sup>4–7</sup> In some CD patients, this bowel wall fibrosis may cause areas of intestinal narrowing (strictures) that are refractory to currently available medical therapies, thus requiring surgical resection, surgical stricturoplasty, or endoscopic dilatation.<sup>8,9</sup>

At histopathology, intestinal strictures in CD can be predominantly inflammatory, predominantly fibrotic, or due to a mixture of both inflammation and fibrosis.<sup>10</sup> The

View this article online at [wileyonlinelibrary.com](http://wileyonlinelibrary.com). DOI: 10.1002/jmri.24815

Received Sep 19, 2014, Accepted for publication Nov 12, 2014.

\*Address reprint requests to: J.R.D., University of Michigan Health System, C.S. Mott Children's Hospital, Department of Radiology, Section of Pediatric Radiology, 1540 East Hospital Dr., Ann Arbor, MI 48109. E-mail: [jonadill@med.umich.edu](mailto:jonadill@med.umich.edu)

From the <sup>1</sup>Section of Pediatric Radiology, Department of Radiology, University of Michigan Health System, Ann Arbor, Michigan, USA; <sup>2</sup>Department of Radiology, University of Michigan Health System, Ann Arbor, Michigan, USA; <sup>3</sup>Division of Gastroenterology, Department of Internal Medicine, University of Michigan Health System, Ann Arbor, Michigan, USA; <sup>4</sup>Department of Pathology, University of Michigan Health System, Ann Arbor, Michigan, USA; and <sup>5</sup>Division of Pediatric Gastroenterology, Department of Pediatrics, University of Michigan Health System, Ann Arbor, Michigan, USA

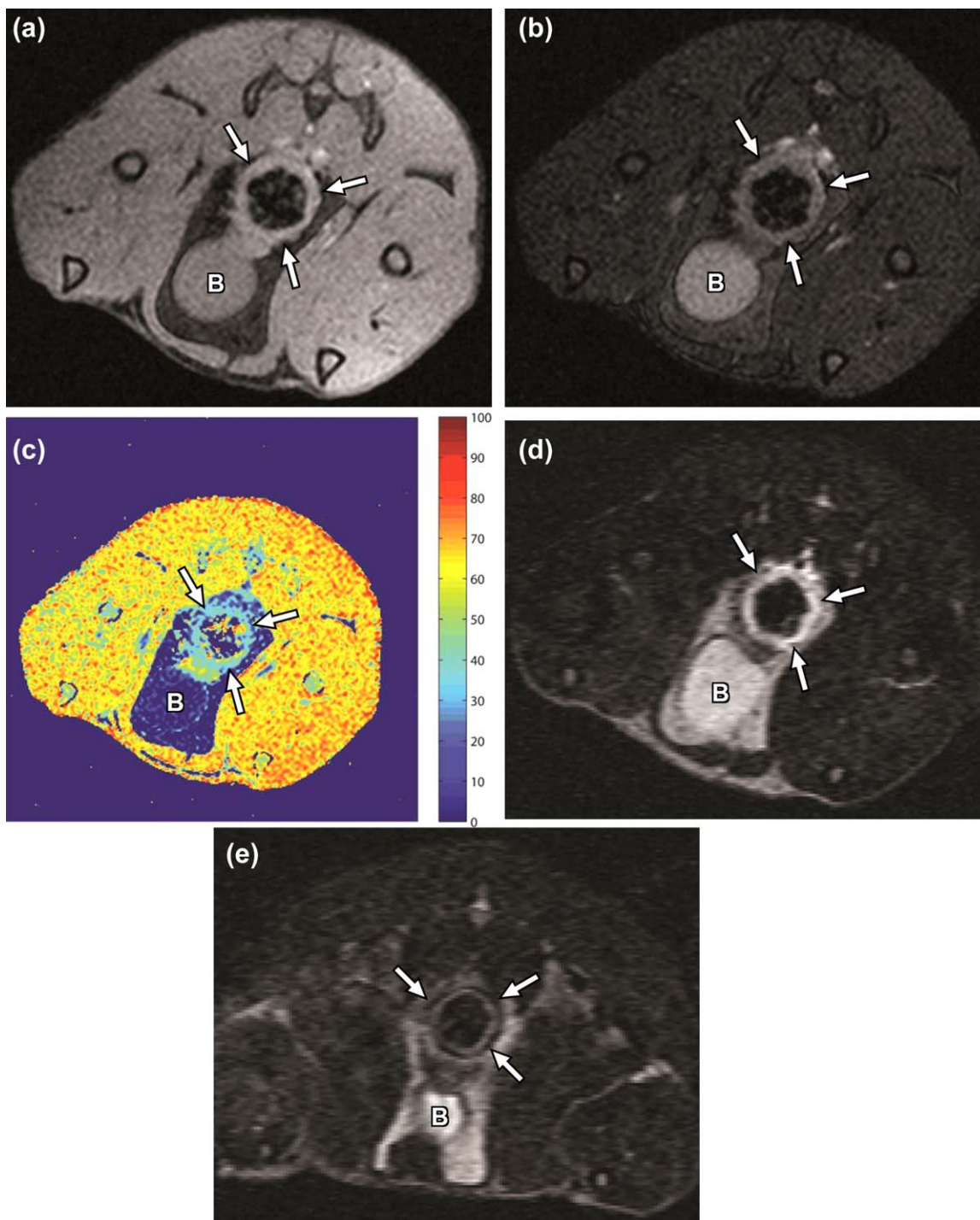


**FIGURE 1:** A,B: Axial MT-MRI images through the distal colon (arrows) without and with 10 kHz off-resonance pulse in a Group 1 animal (purely inflamed bowel). C: Axial parametric map displays calculated MT ratios (MTR from 0 to 100%) for the bowel wall and paraspinous muscles. Muscle and bowel wall show magnetization transfer (MT) effect (skeletal muscle greater than bowel), while fat and fluid in the urinary bladder show none. D,E: Axial  $T_2$ -weighted spin-echo images from individual Group 1 and Group 2 rats, respectively. D: Marked bowel wall signal hyperintensity presumably due to inflammation (arrows), while (E) shows relatively lower bowel wall signal intensity presumably due to fibrosis (arrows; even though there is histologic evidence of extensive superimposed inflammation in this animal). The bowel wall in (E) has a layered appearance, with the outer portion of the bowel wall (corresponding to muscularis propria) having relatively lower signal intensity compared to the inner portion. B = urinary bladder.

ability to reliably, noninvasively characterize strictures could directly impact CD patient management, as predominantly inflammatory strictures commonly respond to medical

immunosuppressive and antiinflammatory therapies, whereas strictures containing substantial fibrosis (either mixed or predominantly fibrotic) are often managed using surgical or

**TABLE 1. Histologic Inflammation and Fibrosis Scoring Systems.**

| Scoring system           | Description  |
|--------------------------|--|
| Acute Inflammation Score |  |
| 0 (none)                 | No inflammation  |
| 1 (mild)                 | Few neutrophils in mucosa/submucosa; no transmural injury or necrosis  |
| 2 (moderate)             | Many neutrophils in mucosa/submucosa; no transmural injury or necrosis   |
| 3 (severe)               | Neutrophils in all layers of the bowel wall; transmural injury or necrosis   |
| Fibrosis Score           |  |
| 0 (none)                 | No architectural distortion; no abnormal Masson's trichrome staining   |
| 1 (mild)                 | No architectural distortion; abnormal Masson's trichrome staining in <50% histopathologic layers                       |
| 2 (moderate)             | No architectural distortion; abnormal Masson's trichrome staining in >50% histopathologic layers                       |
| 3 (severe)               | Architectural distortion of the muscularis propria; abnormal Masson's trichrome staining in all histopathologic layers |

endoscopic therapies.<sup>8,9,11,12</sup> Unfortunately, currently available imaging methods have limitations when trying to determine if areas of intestinal narrowing in CD contain fibrosis. In a study by Adler et al,<sup>10</sup> histologic fibrosis and inflammation were found to be correlated in intestinal strictures, and "strictures on CT enterography (CTE) with the most disease activity also had the most fibrosis on histology."

Of regularly used radiologic modalities, it is conceivable that magnetic resonance imaging (MRI) has the best chance of detecting fibrosis in intestinal strictures in CD patients. This is because this imaging modality permits image creation based on numerous forms of contrast.<sup>13</sup> While image contrast can be obtained using exogenous intravenously administered gadolinium chelates, these contrast agents have drawbacks, including added cost to the examination, risk of nephrogenic systemic fibrosis (NSF) in patients with substantial (individuals with estimated glomerular filtration rate <30 mL/min/1.73 m<sup>2</sup>, in particular) renal dysfunction, and low risk of allergic-like reaction.<sup>14</sup> Numerous MRI techniques are also available that provide image contrast based on endogenous tissue characteristics (eg,  $T_1$  relaxation,  $T_2$  relaxation, diffusion of water). A review of the literature shows a small number of studies describing the use of magnetization transfer MRI (MT-MRI) and  $T_2$ -weighted imaging for detection of bowel wall fibrosis.<sup>15-19</sup> However, there is a paucity of data comparing these two different MRI techniques, including in the setting of superimposed intestinal inflammation.

The purpose of our study was to compare the diagnostic performances of two different quantitative noncontrast MRI techniques, MT-MRI and  $T_2$ -weighted signal intensity ( $T_2$ WSI) ratios, for detecting bowel wall fibrosis in the setting of superimposed intestinal inflammation in a CD animal model.

## Materials and Methods

All rodent procedures were approved by our institutional Committee on the Use and Care of Animals and complied with the National Institutes of Health *Guide for Care and Use of Laboratory Animals*. Ten Lewis rats ("Group 1") received a single trinitrobenzenesulfonic acid (TNBS)-ethanol enema (15 mg TNBS in 50% ethanol) in order to induce inflammation and narrowing of the distal colon and rectum. An additional 10 rats ("Group 2") received five weekly enemas of TNBS-ethanol with escalating TNBS doses (15 to 60 mg) in order to induce both inflammation and fibrosis as well as narrowing of the distal colon and rectum (thus, mimicking human CD), as it is well established that recurrent TNBS-ethanol enemas cause multiple cycles of colitis and bowel wall healing that culminate in transmural intestinal fibrosis.<sup>20</sup> Each enema delivered 250  $\mu$ L of TNBS-ethanol ~7 cm into the rat colon using a pediatric (5 French) feeding tube. One animal in Group 2 died prior to imaging.

Imaging of the colon was performed in each animal cohort 2 days after the final enema using a 2.0-T clear-bore MR system (Varian Unity/Inova, Palo Alto, CA) equipped with actively shielded Acustar gradients (Fig. 1). Images were acquired using a 50 mm diameter, 80 mm length Alderman-Grant slotted cylinder RF probe, and imaging was performed under general anesthesia using isoflurane. After localizer imaging, MT-MRI was performed using a gradient recalled-echo pulse sequence (TR = 200; TE = 3 msec; flip angle = 20 degrees; slice thickness = 2 mm; in-plane resolution = 0.33  $\times$  0.33 mm; number of signal averages = 4; MT pulse = 15 msec Gaussian [1200° flip] applied to each phase encode at 5 kHz and 10 kHz off-resonance). Axial imaging was performed through the rat pelvis and mid-abdomen in order to image the rectum and distal colon. Both 5 and 10 kHz off-resonance pulses were applied in order to generate the MT effect.  $T_2$ -weighted spin-echo imaging was next performed using similar anatomic coverage (TR = 2000 msec; TE = 80 msec; slice thickness = 2 mm; in-plane resolution = 0.25  $\times$  0.25 mm; number of signal averages = 2).

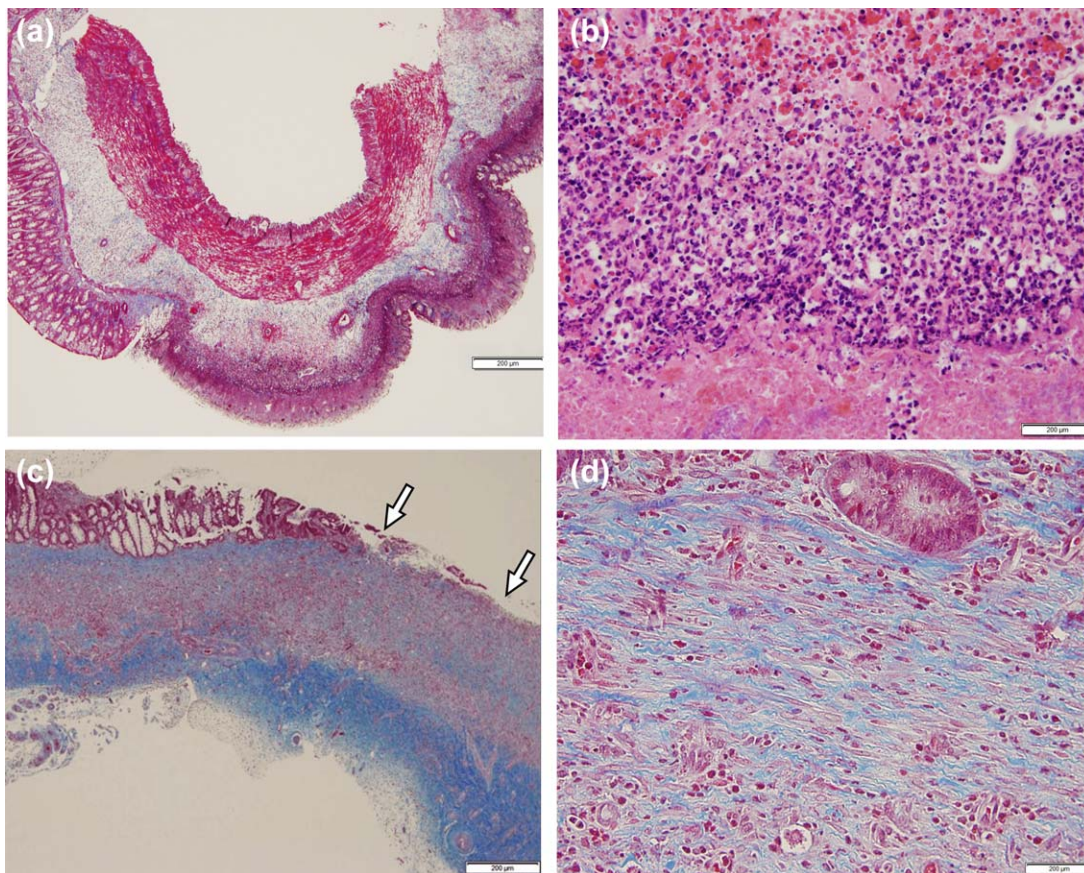


**FIGURE 2: A,B:** Bowel wall histologic images (mucosal surface oriented downward) from a Group 1 rat demonstrate extensive acute inflammation, hemorrhage, and necrosis. The submucosa is expanded, and no abnormal fibrosis is present. **C,D:** Bowel wall histologic images (mucosal surface oriented upward) from a Group 2 rat demonstrate mural thickening with inflammation, transmural fibrosis (blue stain), and mucosal ulceration (arrows).

For each animal, MT ratios (MTR) were calculated using both 5 and 10 kHz off-resonance data in the area of greatest colonic thickening, as determined by a single author (J.R.D., 5 years of experience postfellowship training). MTR was calculated using the following equation:

$$\text{MTR (\%)} = (1 - [M_{\text{sat image}} / M_0 \text{ image}]) \times 100$$

where " $M_{\text{sat image}}$ " is bowel wall signal intensity on images collected with 5 (or 10 kHz) off-resonance RF saturation, and " $M_0 \text{ image}$ " is bowel wall signal intensity on images without RF saturation. MTR was also calculated for paraspinous muscle on the same image that was used to assess the bowel, again using both 5 and 10 kHz off-resonance data. Entire bowel wall regions-of-interest (ROIs) were employed to measure MT signal intensities using MatLab (Natick, MA).

$T_2$ WSI ratio was calculated for each animal in the area of greatest colonic wall thickening by measuring bowel wall signal intensity as well as paraspinous muscle signal intensity on the same image, and then dividing these two measurements. As with MTR, entire bowel wall ROIs placed using MatLab were employed to measure signal intensities.

Animals were euthanized immediately after MRI using inhaled carbon dioxide, and colons were resected in order to obtain

tissue for histopathologic evaluation. Following tissue fixation in formalin and after standard tissue processing, full-thickness tissue specimens from the distal colon and rectum were embedded in paraffin. Representative 5  $\mu\text{m}$  sections were then mounted on glass slides and stained using hematoxylin and eosin (Histology and Immunoperoxidase Laboratory, University of Michigan) as well as Masson's trichrome (McClinchey Histology Lab, Inc.). Colorectal histologic specimens were scored in a blinded fashion by a fellowship-trained gastrointestinal pathologist (D.S.M., 3 years of experience postfellowship training) for histologic inflammation and fibrosis using previously described scoring systems (both inflammation and fibrosis were scored 0–3) (Table 1).<sup>21–23</sup>

Bowel wall collagen protein was isolated from full-thickness colorectal tissue, as previously described.<sup>23</sup> Collagen was quantitated by western blotting using a rabbit-polyclonal antibody against collagen type I (Rockland, Gilbertsville, PA) and normalized to glyceraldehyde-3-phosphate dehydrogenase (GAPDH, an enzyme required for glycolysis and the breakdown of glucose).<sup>23</sup> Autoradiographs were digitally scanned and quantified using ImageJ analysis software.<sup>24</sup>

### Statistical Analysis

Continuous data were summarized using means and standard deviations and box-and-whisker plots were created. Categorical data

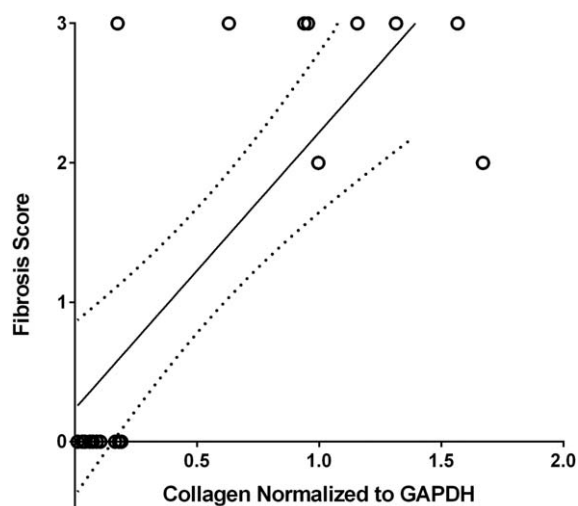


FIGURE 3: Scatterplot with fit line (solid; 95% confidence interval shown as dotted lines) displaying the relationship between bowel wall collagen content based on the western blot method and histologic fibrosis score ( $\rho = 0.76$ ;  $P = 0.0002$ ).

were summarized using counts and percentages. Pearson correlation ( $r$ ) was used to explore the relationship between continuous variables, while Spearman correlation ( $\rho$ ) was used to explore the relationship between continuous and discrete variables. Bowel wall MTR, bowel wall MTR normalized to paraspinous muscle MTR ("normalized MTR"), and  $T_2$ WSI ratios were compared between animal groups using Student's  $t$ -test. Receiver operating characteristic (ROC) curve analyses were performed to compare diagnostic performances. Sensitivity and specificity for detection of bowel wall fibrosis were calculated as were positive likelihood ratios. In addition, the diagnostic performance of a novel parameter—bowel wall  $T_2$ WSI ratio divided by normalized MTR using a 10 kHz off-resonance pulse (" $T_2$ WSI/MTR")—was also evaluated.

$P < 0.05$  was considered statistically significant. Statistical analyses were performed using GraphPad Prism 6 (GraphPad Software, La Jolla, CA).

## Results

### Bowel Wall Histologic Scoring and Collagen Quantification

Histologic scoring of colons showed similar amounts of bowel wall inflammation in each animal group (3.0 for Group 1 vs. 3.0 for Group 2;  $P = 1.0$ ). Group 1 had a mean fibrosis score of 0.0 compared to 2.78 for Group 2 ( $P < 0.0001$ ) (Fig. 2).

Group 1 had a bowel wall mean collagen content of  $0.10 \pm 0.06$  compared to  $1.05 \pm 0.46$  for Group 2 ( $P = 0.0002$ ). There was a significant positive correlation between bowel wall collagen content and histologic fibrosis score, with  $\rho = 0.76$  ( $P = 0.0002$ ) (Fig. 3).

### Bowel Wall MTR and Normalized MTR

At 5 kHz off-resonance, bowel wall mean MTR for Group 1 was  $34.7 \pm 5.2\%$  compared to  $40.3 \pm 3.6\%$  for Group 2

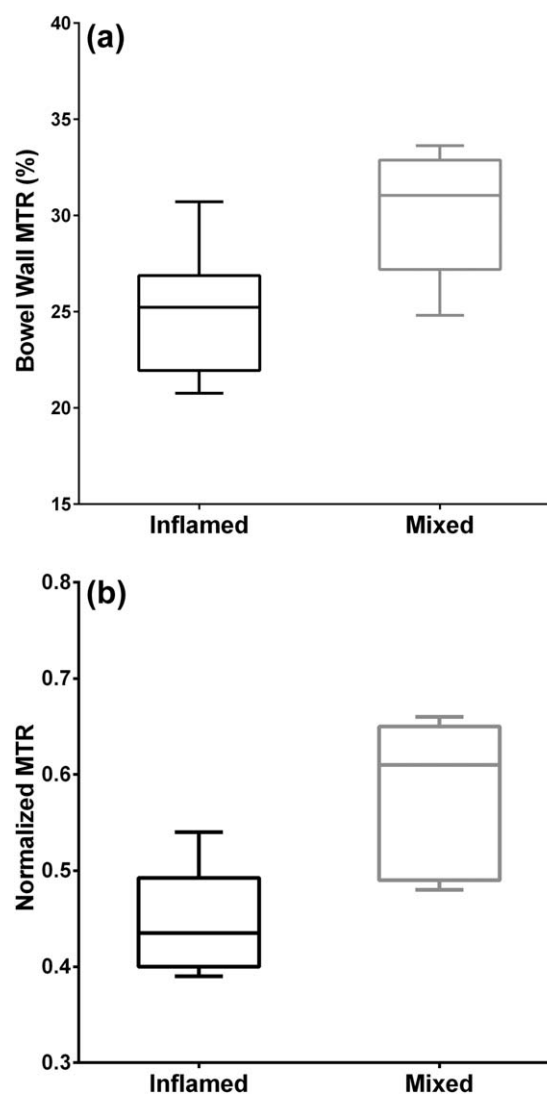


FIGURE 4: **A:** Box-and-whisker plot showing bowel wall MTRs using 10 kHz off-resonance pulse for animals with inflamed (Group 1) and mixed inflammatory and fibrotic (Group 2) bowel segments ( $P = 0.001$ ). **B:** Box-and-whisker plot showing bowel wall MTR normalized to paraspinous muscle MTR using 10 kHz off-resonance pulse for animals with inflamed (Group 1) and mixed inflammatory and fibrotic (Group 2) bowel segments ( $P = 0.0003$ ).

( $P = 0.015$ ). Mean normalized MTR was  $0.53 \pm 0.08$  for Group 1 and  $0.64 \pm 0.07$  for Group 2 ( $P = 0.003$ ).

At 10 kHz off resonance, bowel wall mean MTR for Group 1 was  $24.8 \pm 3.1\%$  compared  $30.3 \pm 3.2\%$  for Group 2 ( $P = 0.001$ ). Mean normalized MTR was  $0.45 \pm 0.05$  for Group 1 and  $0.58 \pm 0.08$  for Group 2 ( $P = 0.0003$ ) (Fig. 4).

There was only weak-to-moderate linear correlation between bowel wall collagen content and normalized MTR using a 10 kHz off-resonance pulse ( $r = 0.35$ ;  $P = 0.15$ ). Scatterplot inspection showed that the relationship between collagen and MTR may not be linear, although MTR increased with increasing collagen up to a certain amount. At the highest levels of bowel wall collagen, MTR was noted to decrease. Similar patterns were observed for both

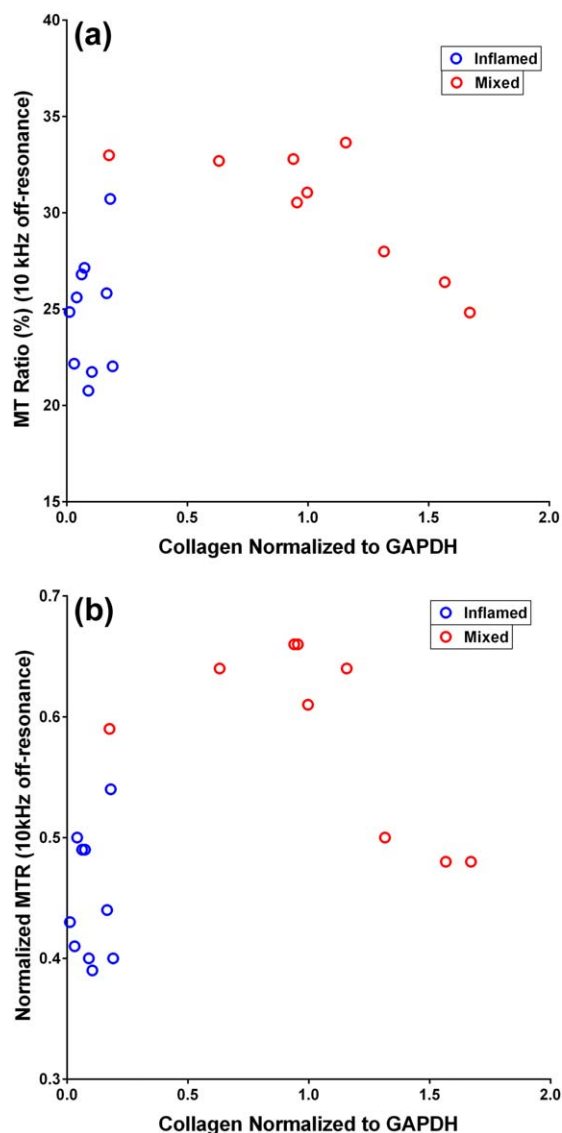


FIGURE 5: A: Scatterplot showing the relationship between bowel wall collagen vs. MTR using a 10 kHz off-resonance pulse. B: Scatterplot showing the relationship between bowel wall collagen vs. normalized MTR using a 10 kHz off-resonance pulse shows a similar pattern.

nonnormalized and normalized 5 and 10 kHz off-resonance data (Fig. 5).

### $T_2$ WSI Ratio

Bowel wall mean  $T_2$ WSI ratio was  $5.32 \pm 0.98$  for Group 1 and  $3.01 \pm 0.66$  for Group 2 ( $P < 0.0001$ ) (Fig. 6). There were moderate-strong negative linear correlations between  $T_2$ WSI ratio and normalized MTR ( $r = -0.63$ ;  $P = 0.004$ ) and between  $T_2$ WSI ratio and bowel wall collagen content ( $r = -0.7$ ;  $P = 0.0009$ ) (Fig. 7).

### ROC Curve Analyses

Bowel wall MTRs demonstrated ROC areas-under-the-curve (AUC) of 0.81 at 5 kHz and 0.88 at 10 kHz off-resonance, respectively, for discriminating purely inflamed

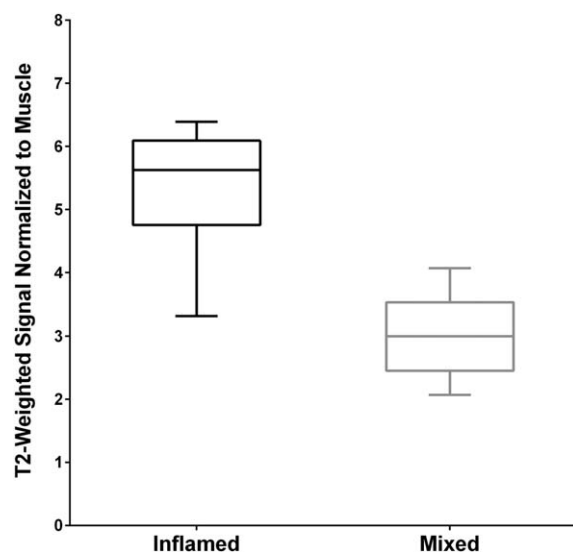


FIGURE 6: Box-and-whisker plot showing bowel wall  $T_2$ -weighted signal intensity ( $T_2$ WSI) normalized to paraspinous muscle signal intensity for animals with inflamed (Group 1) and mixed inflammatory and fibrotic (Group 2) strictures ( $P < 0.0001$ ).

from mixed inflammatory and fibrotic colon. Normalized MTRs demonstrated ROC AUC of 0.88 at 5 kHz and 0.89 at 10 kHz off-resonance, respectively.  $T_2$ WSI ratios demonstrated the best diagnostic performance for discrimination of Group 2 from Group 1 animals, with an ROC AUC of 0.97 (Fig. 8).

MTR, normalized MTR, and  $T_2$ WSI ratio sensitivities, specificities, and positive likelihood ratios for discriminating bowel segments with both inflammation and fibrosis (Group 2) from those with only inflammation (Group 1) were calculated and are presented in Table 2.

The diagnostic performance of a novel parameter—bowel wall  $T_2$ WSI ratio divided by normalized MTR using a 10 kHz off-resonance pulse (" $T_2$ WSI/MTR")—was also assessed (Fig. 9). The mean of this novel parameter was  $12.06 \pm 2.70$  for Group 1 and  $5.22 \pm 1.29$  for Group 2 ( $P < 0.0001$ ). ROC AUC for this novel parameter for detecting bowel wall fibrosis was 0.98. Parameter sensitivity, specificity, and positive likelihood ratio are presented in Table 2.

### Discussion

MRI using a magnetization transfer technique (MT-MRI) allows image contrast to be generated based on the interactions between the protons of free water and those of large immobilized macromolecules, such as collagen.<sup>16,25</sup> Image contrast due to the presence of collagen at MT-MRI is most likely because of exchange of protons of hydroxyl and amino groups and water and related exchange of longitudinal magnetization.<sup>26</sup> It has been theorized that the presence of bowel wall fibrosis should cause increased MTR.<sup>16</sup> This imaging technique, while not used commonly in

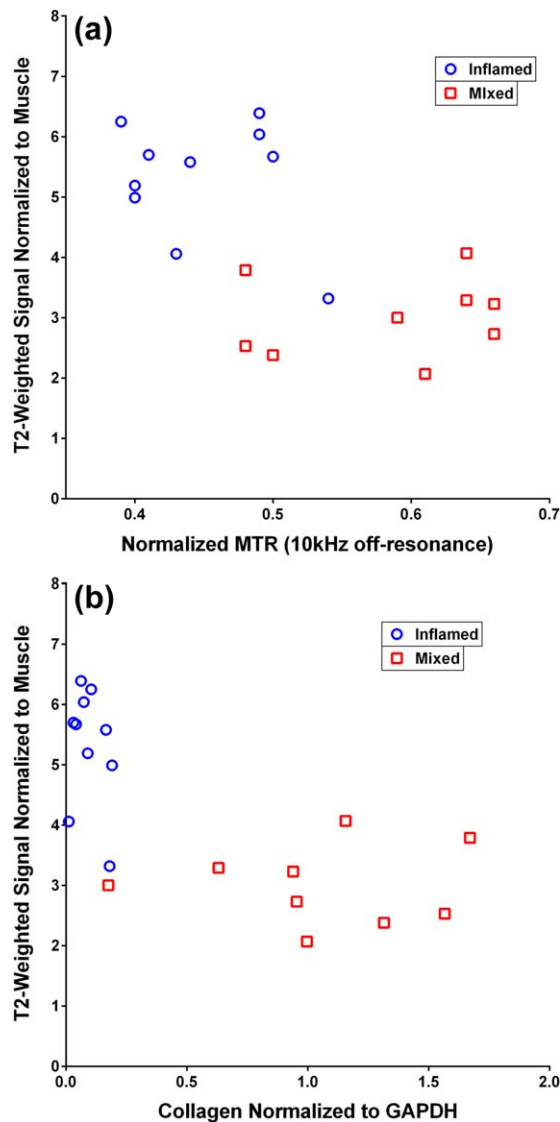


FIGURE 7: **A:** Scatterplot showing the relationship between bowel wall normalized MTR at 10 kHz off-resonance vs.  $T_2$ -weighted signal intensity ( $T_2$ WSI) normalized to paraspinous muscle ( $r = -0.63$ ;  $P = 0.004$ ). Animals in Groups 1 (bowel wall inflammation only) and 2 (mixed inflammation and fibrosis) cluster into two distinct groups. A single Group 1 animal is present in the Group 2 cluster. **B:** Scatterplot showing the relationship between bowel wall collagen content vs.  $T_2$ -weighted signal intensity ( $T_2$ WSI) normalized to paraspinous muscle ( $r = -0.70$ ;  $P = 0.0009$ ). Increased collagen is moderate-to-strongly correlated with decreased bowel wall  $T_2$ -weighted signal intensity.

routine clinical MRI in the abdomen or pelvis, is available on most clinical MRI scanners, and imaging can be performed using a fast imaging techniques, such as a breath-hold gradient recalled-echo pulse sequence. Our results confirm those previously published by Adler et al,<sup>16</sup> who found that MT-MRI is "sensitive to bowel wall fibrosis as occurs in Crohn's strictures." In their study, the bowel wall MTR of rats with fibrosis was higher than the MTR of control animals and animals with bowel wall inflammation but no fibrosis.

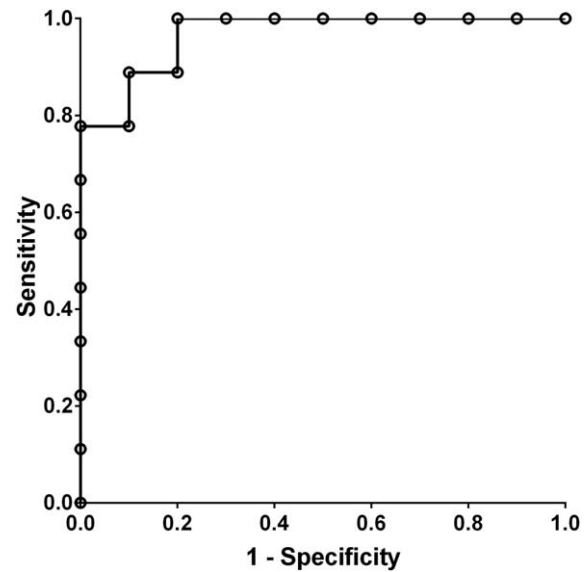


FIGURE 8: ROC curve for discrimination of mixed inflammatory and fibrotic bowel segments (Group 2 animals) from purely inflamed bowel segments (Group 1 animals) using bowel wall  $T_2$ -weighted signal intensity ( $T_2$ WSI) ratios. AUC is 0.97, consistent with excellent diagnostic performance.

Our study corroborates the results of Adler et al<sup>16</sup> using an entirely different CD animal model. The rodent model used in the Adler et al<sup>16</sup> investigation used subserosal injections of peptidoglycan-polysaccharide to cause inflammation of the cecum and eventual intestinal fibrosis, whereas our rodent model used TNBS-ethanol enemas to cause inflammation and eventual fibrosis of the distal colon and rectum.<sup>27,28</sup> When comparing bowel wall MTR in animals with inflammation only to animals with mixed inflammation and fibrosis, we were able to show similar significant results using both 5 kHz and 10 KHz off-resonance pulses. Upon normalizing bowel wall MTR to skeletal muscle MTR, even better discrimination between animal groups was able to be achieved with even greater statistical significance.

Bowel wall  $T_2$ WSI ratios were also significantly different between animals with purely inflammatory lesions and animals with mixed inflammatory and fibrotic lesions. Purely inflammatory animals showed significantly higher  $T_2$ WSI ratios than animals with mixed lesions. This is presumably because the extensive bowel wall fibrosis in the latter animal group, which was confirmed by bowel wall histologic evaluation and collagen quantification, causes  $T_2$  shortening and associated signal loss. Fibrosis is well known to lower  $T_2$ -weighted signal intensity, although there is little known about how fibrosis affects bowel wall signal intensity in the setting of superimposed inflammation. These results suggest that mixed strictures in human CD may well have lower  $T_2$ -weighted signal intensities when normalized to muscle signal intensity than purely inflamed strictures, although the diagnostic performance of this ratio has yet to

**TABLE 2. Sensitivities, Specificities, and Positive Likelihood Values of Magnetization Transfer Ratio (MTR), Normalized MTR, and  $T_2$ -Weighted Signal Intensity ( $T_2$ WSI) Ratios for Discriminating Mixed Inflamed and Fibrotic From Purely Inflamed Bowel Segments**

| Noncontrast MRI technique  | Sensitivity | Specificity | Positive likelihood ratio | Cutoff value |
|----------------------------|-------------|-------------|---------------------------|--------------|
| MTR - 5 kHz off-resonance  | 67%         | 90%         | 6.67                      | >40.4        |
| MTR - 10 kHz off-resonance | 78%         | 90%         | 7.78                      | >27.6        |
| Normalized MTR (5 kHz)     | 67%         | 90%         | 6.67                      | >0.63        |
| Normalized (10 kHz)        | 67%         | 90%         | 6.67                      | >0.52        |
| $T_2$ WSI Ratio            | 89%         | 90%         | 8.89                      | <3.93        |
| $T_2$ W/MTR parameter      | 100%        | 90%         | 10.0                      | <8.65        |

MTR = magnetization transfer ratio; kHz = kilohertz;  $T_2$ WSI =  $T_2$ -weighted signal intensity;  $T_2$ W/MTR =  $T_2$ -weighted signal intensity divided by normalized magnetization transfer ratio using a 10 kHz off-resonance pulse.

be established in clinical practice. Interestingly, the colons of several fibrotic animals also showed a clear layered appearance, with the outer portion of the bowel wall having relatively lower signal intensity than the inner portion. Additional study is needed to establish the significance of this observation, as evaluation of the bowel wall for a layered appearance was not a formally assessed outcome.

Based on bowel wall collagen quantification using the western blot method, we demonstrated that as collagen increased,  $T_2$ WSI ratios decreased. Scatterplot inspection showed that the loss of bowel wall  $T_2$ -weighted signal intensity occurred at relatively low collagen concentrations and then plateaued (perhaps a "floor effect"). Further research is

needed to determine if this observation is reproducible. Correlation of MTR with bowel wall collagen showed that MTR increased with increasing collagen to a certain level. However, a decrease in MTR was seen in animals with the greatest amounts of collagen. This finding is of uncertain origin, and more research is needed to determine if this observation is correct.

When comparing the diagnostic performances of bowel wall MTR using 5 and 10 kHz off-resonance pulses, normalized MTR using 5 and 10 kHz off-resonance pulses, and  $T_2$ WSI ratios, there are several interesting observations. First, three of four MT-MRI techniques, including bowel wall MTR using a 10 kHz off-resonance pulse as well as normalized MTR using 5 and 10 kHz off-resonance pulses, have similar diagnostic performances. Second, bowel wall  $T_2$ WSI ratios, which can be very easily calculated on routine clinical  $T_2$ -weighted images, seem to have better diagnostic performance than MTR, with an ROC AUC of 0.97. Visual inspection of our data using a scatterplot of normalized MTR (using a 10 kHz off-resonance pulse) vs.  $T_2$ WSI ratios shows that 18 of our 19 animals that survived to imaging cluster into two very distinct cohorts that make sense based on histology and MRI physics. Group 1 animals, those with purely inflammatory lesions, have high bowel wall  $T_2$ WSI ratios and low normalized MTR, whereas Group 2 animals, those with mixed inflammatory and fibrotic lesions, have relatively low  $T_2$ WSI ratios and relatively high normalized MTR.

Based on this observed clustering, a novel parameter— $T_2$ WSI ratio divided by normalized MTR using a 10 kHz off-resonance pulse (" $T_2$ WSI/MTR")—was devised. This parameter actually demonstrated better diagnostic performance than MT-MRI or  $T_2$ WSI ratios alone, and it allowed the best discrimination between fibrotic (Group 2) and non-fibrotic (Group 1) animals. In clinical practice when imaging actual human CD patients, we propose that high-

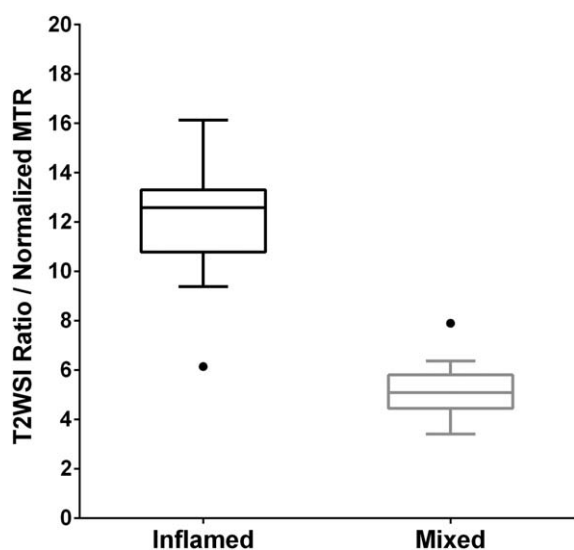


**FIGURE 9:** Box-and-whisker plot showing the novel parameter: bowel wall  $T_2$ -weighted signal intensity ( $T_2$ WSI) ratio divided by normalized MTR (using a 10 kHz off-resonance pulse), or " $T_2$ W/MTR," for inflamed (Group 1) and mixed inflammatory and fibrotic (Group 2) colon ( $P < 0.0001$ ). Dots represent statistical outliers (greater than 1.5 interquartile ranges below first quartile or above third quartile).



quality, targeted  $T_2$ -weighted imaging and MT-MRI be performed through any area of disease demonstrating bowel wall thickening, luminal narrowing, and upstream dilatation in order to optimize both signal-to-noise ratio and spatial resolution as well as facilitate ROI placement. These findings, together, suggest the presence of an obstructing stricture that would benefit from bowel wall tissue characterization (ie, is there fibrosis?). Based on the known distribution of CD, these strictures are most likely to involve the distal or terminal ileum, although there is no reason why strictures involving other portions of the intestine cannot be characterized by MRI. While the colon is commonly filled with fecal material (especially upstream to an obstructing stricture), portions causing bowel obstruction (with associated substantial wall thickening and luminal narrowing) are generally well visualized by MRI and can probably be characterized without a formal pre-MRI colon cleansing regimen.

Our study has a few limitations to be acknowledged. First, imaging was performed on a CD animal model and not human CD patients. While a particular advantage of our animal model is that it allows transmural histologic evaluation of the colon immediately after MRI, these non-contrast MRI techniques must be further assessed in vivo in human CD patients with intestinal strictures just prior to surgery in order to obtain one-to-one MRI-histopathology correlation. Second, further investigations are required to determine the true sensitivities and specificities of these bowel wall imaging techniques in humans. We do not know if one technique, both techniques combined (eg, novel  $T_2$ WSI/MTR parameter), or neither technique is sensitive for detecting small amounts of bowel wall fibrosis or progression of bowel wall fibrosis over time. Also, it is very possible that the relationships between fibrosis/collagen and both MTR and  $T_2$ WSI ratios are complex and nonlinear. It is reassuring that a recent study by Pazahr et al<sup>29</sup> performed to assess the feasibility of MT-MRI in human CD patients found that MTR was significantly increased in bowel wall segments with fibrotic scarring.

Finally, numerous additional studies, which will likely be in vitro, in vivo in animals, as well as in vivo in humans, are needed to completely optimize pulse sequences used to obtain MT-MRI and  $T_2$ WSI data in order to maximize the clinical utility of these techniques. For example, MT imaging can be performed in conjunction with several routinely employed clinical pulse sequences (eg, gradient recalled-echo vs. balanced steady-state free precession) and using a wide range of off-resonance pulses (eg, 5 vs. 10 kHz); we do not know which pulse sequence or off-resonance frequency will offer the greatest sensitivity and specificity for detecting bowel wall fibrosis.  $T_2$ -weighted imaging of the bowel also can be performed using a variety of routine clinical pulse sequences (eg, single-shot fast spin-

echo vs. fast spin-echo) with many associated parameters that require optimization as well.

In conclusion, both MT-MRI and  $T_2$ WSI ratios, two different quantitative noncontrast MRI techniques that rely on endogenous tissue contrast, allow detection of bowel wall fibrosis in the setting of superimposed inflammation in a CD animal model. Upon direct comparison, our data suggest that  $T_2$ WSI ratios offer better diagnostic performance for discriminating inflamed from mixed inflammatory and fibrotic strictures than MT-MRI based on ROC curve analysis. A novel parameter—bowel wall  $T_2$ WSI ratio divided by normalized MTR—also offers excellent diagnostic performance and may be better than MT-MRI or  $T_2$ WSI ratios alone. Additional studies are necessary to further optimize these MRI techniques for the detection of bowel wall fibrosis and discrimination of fibrosis from inflammation as well as to assess their individual and combined clinical utilities in humans with stricturing CD.

---

## Acknowledgments

Contract grant sponsor: National Center for Advancing Translational Sciences; Contract grant number: 2UL1TR000433. The content is solely the responsibility of the authors and does not necessarily represent the official views of NCATS or the National Institutes of Health.

---

## References

1. Kappelman MD, Rifas-Shiman SL, Porter CQ, et al. Direct health care costs of Crohn's disease and ulcerative colitis in US children and adults. *Gastroenterology* 2008;135:1907–1913.
2. Bodger K. Cost of illness of Crohn's disease. *Pharmacoeconomics* 2002;20:639–652.
3. Loftus EV Jr, Schoenfeld P, Sandborn WJ. The epidemiology and natural history of Crohn's disease in population-based patient cohorts from North America: a systematic review. *Aliment Pharmacol Ther* 2002;16:51–60.
4. Dhillon S, Loftus E, Tremaine W, et al. The natural history of surgery for Crohn's disease in a population-based cohort from Olmsted County, Minnesota. *Am J Gastroenterol* 2005;100:S303, Abstract 819.
5. Lichtenstein GR, Olson A, Travers S, et al. Factors associated with the development of intestinal strictures or obstructions in patients with Crohn's disease. *Am J Gastroenterol* 2006;101:1030–1038.
6. Loftus CG, Loftus EV Jr, Harmsen WS, et al. Update on the incidence and prevalence of Crohn's disease and ulcerative colitis in Olmsted County, Minnesota, 1940–2000. *Inflamm Bowel Dis* 2007;13:254–261.
7. Oberhuber G, Stangl PC, Vogelsang H, et al. Significant association of strictures and internal fistula formation in Crohn's disease. *Virchows Arch* 2000;437:293–297.
8. Cosnes J. Can we modulate the clinical course of inflammatory bowel diseases by our current treatment strategies? *Dig Dis* 2009;27:516–521.
9. Jones DW, Finlayson SR. Trends in surgery for Crohn's disease in the era of infliximab. *Ann Surg* 2010;252:307–312.
10. Adler J, Punglia DR, Dillman JR, et al. Computed tomography enterography findings correlate with tissue inflammation, not fibrosis in

- resected small bowel Crohn's disease. *Inflamm Bowel Dis* 2012;18:849-856.
11. Paine E, Shen B. Endoscopic therapy in inflammatory bowel diseases (with videos). *Gastrointest Endosc* 2013;78:819-835.
  12. Shaffer VO, Wexner SD. Surgical management of Crohn's disease. *Langenbecks Arch Surg* 2013;398:13-27.
  13. Yacoub JH, Oto A. New magnetic resonance imaging modalities for Crohn disease. *Magn Reson Imag Clin N Am* 2014;22:35-50.
  14. <http://www.acr.org/quality-safety/resources/contrast-manual> (2014) Manual on Contrast Media v9. Accessed on July 31, 2014.
  15. Adler J, Rahal K, Swanson SD, et al. Anti-tumor necrosis factor alpha prevents bowel fibrosis assessed by messenger RNA, histology, and magnetization transfer MRI in rats with Crohn's disease. *Inflamm Bowel Dis* 2013;19:683-690.
  16. Adler J, Swanson SD, Schmiedlin-Ren P, et al. Magnetization transfer helps detect intestinal fibrosis in an animal model of Crohn disease. *Radiology* 2011;259:127-135.
  17. Maccioni F, Staltari I, Pino AR, et al. Value of T2-weighted magnetic resonance imaging in the assessment of wall inflammation and fibrosis in Crohn's disease. *Abdom Imaging* 2012;37:944-957.
  18. Quaia E, Cabibbo B, Sozzi M, et al. Biochemical markers and MR imaging findings as predictors of Crohn disease activity in patients scanned by contrast-enhanced MR enterography. *Acad Radiol* 2014 [Epub ahead of print].
  19. Quencer KB, Nimkin K, Mino-Kenudson M, et al. Detecting active inflammation and fibrosis in pediatric Crohn's disease: prospective evaluation of MR-E and CT-E. *Abdom Imaging* 2103;38:705-713.
  20. Morris GP, Beck PL, Herridge MS, et al. Hapten-induced model of chronic inflammation and ulceration in the rat colon. *Gastroenterology* 1989;96:795-803.
  21. Dillman JR, Stidham RW, Higgins PD, et al. US elastography-derived shear wave velocity helps distinguish acutely inflamed from fibrotic bowel in a Crohn disease animal model. *Radiology* 2013;267:757-766.
  22. Kim K, Johnson LA, Jia C, et al. Noninvasive ultrasound elasticity imaging (UEI) of Crohn's disease: animal model. *Ultrasound Med Biol* 2008;34:902-912.
  23. Stidham RW, Xu J, Johnson LA, et al. Ultrasound elasticity imaging for detecting intestinal fibrosis and inflammation in rats and humans with Crohn's disease. *Gastroenterology* 2011;141:819-826 e811.
  24. Schneider CA, Rasband WS, Eliceiri KW. NIH Image to ImageJ: 25 years of image analysis. *Nat Methods* 2012;9:671-675.
  25. Mehta RC, Pike GB, Enzmann DR. Magnetization transfer magnetic resonance imaging: a clinical review. *Top Magn Reson Imag* 1996;8:214-230.
  26. Swanson SD. Molecular mechanisms of magnetization transfer. In: *Proc 18th Annual Scientific Meeting ISMRM, Stockholm; 2010* (abstract 337).
  27. Neurath M, Fuss I, Strober W. TNBS-colitis. *Int Rev Immunol* 2000;19:51-62.
  28. Johnson LA, Luke A, Sauder K, et al. Intestinal fibrosis is reduced by early elimination of inflammation in a mouse model of IBD: impact of a "top-down" approach to intestinal fibrosis in mice. *Inflamm Bowel Dis* 2012;18:460-471.
  29. Pazahr S, Blume I, Frei P, et al. Magnetization transfer for the assessment of bowel fibrosis in patients with Crohn's disease: initial experience. *MAGMA* 2013;26:291-301.